DISCRETE AND CONTINUOUS
DYNAMICAL SYSTEMS SERIES B

doi:10.3934/dcdsb.2021114

A SHORT-TERM FOOD INTAKE MODEL INVOLVING GLUCOSE, INSULIN AND GHRELIN

Massimo Barnabei

High School Melchiorre Delfico
Teramo, Italy

Alessandro Borri*

CNR-IASI Biomathematics Laboratory
National Research Council of Italy, Rome, Italy

Andrea De Gaetano

CNR-IRIB Institute for Biomedical Research and Innovation
National Research Council of Italy, Palermo, Italy

Costanzo Manes

Department of Information Engineering, Computer Science, and Mathematics
University of L'Aquila, L'Aquila, Italy

Pasquale Palumbo

Department of Biotechnologies and Biosciences
University of Milano-Bicocca, Milan, Italy

Jorge Guerra Pires

Centro de Desenvolvimento Tecnológico em Saúde/Oswaldo Cruz Foundation
Rio de Janeiro, Brazil

(Communicated by Pierre Magal)

Abstract. Body weight control is gaining interest since its dysregulation eventually leads to obesity and metabolic disorders. An accurate mathematical description of the behavior of physiological variables in humans after food intake may help in understanding regulation mechanisms and in finding treatments. This work proposes a multi-compartment mathematical model of food intake that accounts for glucose-insulin homeostasis and ghrelin dynamics. The model involves both food volumes and glucose amounts in the two-compartment system describing the gastro-intestinal tract. Food volumes control ghrelin dynamics, whilst glucose amounts clearly impact on the glucose-insulin system. The qualitative behavior analysis shows that the model solutions are mathematically coherent, since they stay positive and provide a unique asymptotically stable equilibrium point. Ghrelin and insulin experimental data have been exploited to fit the model on a daily horizon. The goodness of fit and the physiologically meaningful time courses of all state variables validate the efficacy of the model to capture the main features of the glucose-insulin-ghrelin interplay.

2020 *Mathematics Subject Classification.* Primary: 92-10, 92B05; Secondary: 93C95.

Key words and phrases. Glucose-insulin system, Mathematical physiology, Energy homeostasis, Ghrelin.

* Corresponding author: Alessandro Borri (e-mail: *alessandro.borri@biomatematica.it*).

1. **Introduction.** The correct balance between food intake and energy consumption in humans is known to be regulated by a wide set of hormones and, nowadays, mathematical models of such a tangled network of molecular players are helping to unravel the many mechanisms involved [2, 28].

In this note we propose a model that aims at connecting food intake, glucose-insulin homeostasis and ghrelin dynamics. Motivation stems from the fact that a correct understanding of the many hormones (besides insulin) and metabolites contributing in plasma glucose regulation may lead to a deeper understanding of dysregulation mechanisms, eventually leading to obesity and metabolic disorders, and may help in designing a safe and efficient artificial pancreas, an issue recently gaining an increasing interest in the control community.

Ghrelin is a peptide hormone produced in the stomach that, if present in a sufficient concentration in humans, gives sensations of hunger and was initially identified as a stimulus for the release of growth hormone [18]. After its discovery, Nakazato et al. [17] were the first to conjecture a role for ghrelin in the regulation of feeding. Several subsequent studies (e.g [3, 4]) suggested that the diurnal rhythm of ghrelin is linked to meal initiation in humans. Indeed, the blood concentration of ghrelin increases before each meal and rapidly decreases after eating. Studies about plasma ghrelin levels after diet-induced weight loss or gastric bypass surgery by Cummings et al. [5, 6] advocate that ghrelin may have also a role in long-term regulation of food intake. Other findings support the concept that the endogenous ghrelin system may have a paramount role in starvation, as a survival hormone that maintains blood glucose and helps preventing loss of body weight [14].

Despite the cited findings about the role of ghrelin in the food-intake process, only few models can be found in the literature that incorporate the hormone. Toghaw et al. [29] in 2012 considered ghrelin in a mathematical model aiming at shedding light into the type-2 diabetes improvement after bariatric surgery. Pires et al. [23] proposed in 2017 a model focused on the short-term dynamics of ghrelin that is grounded in the established physiology and that replicates in vivo data (see also [24]). Uluseker et al. [30] presented in 2018 a multi-level model of glucose homeostasis in which they also included a differential equation describing plasma ghrelin dynamics. In these models, however, the secretion of ghrelin is considered to be inhibited by glucose in the stomach or in the small intestine, whereas important studies suggest that the inhibitory signal arises only from the first part of the small intestine in response to food volume [31, 19].

With the aim of continuing investigations in this direction, a new model is here proposed, which describes the daily dynamics of ghrelin and, at the same time, includes glucose-insulin regulation, taking a step forward towards a complete mathematical description of food intake and metabolic regulation. We consider a multi-compartment model, in which both the food volume and the glucose concentration in the stomach and in the small intestine are taken into account. The presented model provides a basis for more complete mathematical description of the long-term regulation of body weight, which could be achieved considering the action of some other hormones such as leptin, GLP1 and GIP.

2. **Model setting.** The model here presented aims at explaining what happens in the human body after meals, with particular regard to the glucose-insulin system and to the time evolution of ghrelin.

Food transit in the gastrointestinal tract is modeled using two compartments: the first represents stomach and duodenum, the second models the jejunum and the ileum. For simplicity, we will refer to the first compartment as *stomach* and to the second as *jejunum*. Below we provide an accurate description of the desired qualitative behavior of the model, in order to support the proposed model structure.

We denote by S and J the food volume (ml) in the first and second compartments, respectively. After the ingestion, the first part of the gastrointestinal tract starts to fill up and to gradually empty out towards the jejunum and the ileum without significant nutrient absorption, so corresponding to a decrease of S we have an identical increase of J. Then the food leaves the second compartment and reaches the large intestine (not modeled, since it does not play an active role in the regulation of the other model variables). We assume that some gastric and pancreatic/intestinal secretion always occurs (as a first approximation, at a constant rate), i.e. the two compartments never empty completely.

The differential equations describing the gastrointestinal variables S and J are constructed with the aim of modeling the feedback mechanism that slows down the gastric emptying. Indeed, some hormones (e.g. GLP-1, CCK, peptide Y, oxyntomodulin) produced in the jejunum/ileum in response to food transit control the gastrointestinal motility [15, 27, 13]. In particular, we propose a model in which the emptying of the stomach compartment (1) is inhibited by the food volume in the jejunum compartment (2), by means of and emptying rate (3) that depends on $J(t)$:

$$\dot{S}(t) = -\eta K_{JS}(t)S(t) + k_S + F(t) \tag{1}$$

$$\dot{J}(t) = \eta(K_{JS}(t)S(t) - k_{XJ}J(t)) + k_J \tag{2}$$

$$K_{JS}(t) = k_{JS}^{max}\mathrm{e}^{-\lambda_{JS}J(t)} \tag{3}$$

where $F(t)$, $[ml/min]$, is the food ingestion rate, k_{JS}^{max}, $[min^{-1}]$, is the maximum rate transfer from stomach to jejunum, λ_{JS}, $[ml^{-1}]$, is the rate of decay of stomach-jejunal transfer with jejunum filling, k_{XJ}, $[min^{-1}]$, is the rate of jejunal emptying, k_S, k_J, $[ml/min]$, are the gastric and jejunal secretions flow rates. η is a dimensionless coefficient in $(0, 1]$ included to take into account the fact that the food transit time in the gastrointestinal tract is also influenced by the type of ingested food [9, 16]. Thus, η should depend on the composition of the meal. In this work, without loss of generality we assume $\eta = 1$.

Making the simplifying assumption that the food ingestion rate is constant and the same during the three meals (breakfast, lunch, and dinner), $F(t)$ takes the form

$$F(t) = \begin{cases} r, & t \in [t_b, t_b + \tau_b] \cup [t_l, t_l + \tau_l] \cup [t_d, t_d + \tau_d] \\ 0, & otherwise \end{cases} \tag{4}$$

in which t_b, t_l and t_d are the starting times and τ_b, τ_l and τ_d are the meal durations. The aforementioned model for food volumes is inherited from [23]: besides a different shape for the feedback on gastric emptying, the main difference is the presence of a constant basal secretion that prevents the complete emptying of both compartments.

The glucose absorption after a meal is described using a two-compartment model parallel to the the one used for the food transit. Let G_S and G_J, both in $(mmol)$, denote the glucose amounts in the two compartments. The filling of first compartment depends on the glucose content of the meal. Then glucose reaches the second

compartment where it is either absorbed or moved to the large intestine. We assume that the glucose transit rates between the two compartments are the same as for the food volumes.

The process that brings ingested glucose to be available in blood consists of several phases and it is still under investigation. It starts in the gastrointestinal tract with carbohydrates digestion by salivary and pancreatic amylases, then glucose is absorbed by the intestinal enterocytes through secondary active transport, thanks to the action of the sodium-glucose cotransporter (SGLT1) and it exits across the basolateral membrane of the enterocytes using the facilitated glucose transporter GLUT2 [32, 33]. Other mechanisms have also been taken into account to explain the intestinal absorption of glucose [33]; in particular some studies [11, 12] claim that a facilitated diffusive component exists and is mediated by the glucose-induced recruitment of GLUT2 to the brush-border membrane, but this hypothesis is contradicted by some other findings [25]. We consider glucose to be absorbed into blood from the second compartment, depending on the sugar in its lumen, and that such transfer is driven by luminal glucose concentration rather than mass [8].

With regards to plasma insulin and glucose, we know that the increase of insulin concentration follows the increase of glycaemia, with some delay [20]. In essence, the plasma glucose prompts the secretion of the granular insulin ready for release at the β-cell membrane rather than causing a direct increase of plasma insulin. Granular insulin R $(pmol)$ is released with a rate that depends on the glucose concentration in plasma, inducing an increase of the concentration of plasma insulin I (pM). Plasma glucose G (mM) is reduced due to the insulin-mediated absorption by tissues, depending on insulin sensitivity, whereas it increases due to hepatic glucose production, which we assume constant, and to the glucose G_J absorbed from the intestine. The above qualitative description is mathematically represented by the following equations:

$$\dot{G_S}(t) = -\eta K_{JS}(t) G_S(t) + \rho_{GM} F(t) \tag{5}$$

$$\dot{G_J}(t) = \eta(K_{JS}(t) G_S(t) - k_{XJ} G_J(t)) - k_{GJ} \frac{G_J(t)}{J(t)} \tag{6}$$

$$\dot{G}(t) = \frac{k_G}{V_G} - k_{XGI} I(t) G(t) + k_{GJ} \frac{G_J(t)}{J(t) V_G} \tag{7}$$

$$\dot{I}(t) = -k_{XI} I(t) + k_{IRG} \left(\frac{G(t)}{G_b} \right)^{\gamma_{IRG}} \frac{R(t)}{V_I} \tag{8}$$

$$\dot{R}(t) = k_{RG} G(t) - k_{IRG} \left(\frac{G(t)}{G_b} \right)^{\gamma_{IRG}} R(t) \tag{9}$$

where ρ_{GM}, $[mmol/ml]$, is the glucose density of food, k_{GJ}, $[ml/min]$, is the glucose clearance rate from jejunum to bloodstream, k_G, $[mmol/min]$, is the hepatic glucose output, V_G, $[l]$, is the glucose distribution volume, k_{XGI}, $[pM^{-1}min^{-1}]$, is the insulin sensitivity, k_{IRG}, $[min^{-1}]$, is the rate of insulin release from granules with increasing glycaemia, G_b, $[mM]$, is the basal glycemia, γ_{IRG}, $[-]$, is the exponent of the supralinear increase of insulin release from granules with increasing glycaemia, V_I, $[l]$, is the insulin distribution volume, k_{XI}, $[min^{-1}]$, is the insulin elimination rate, k_{RG}, $[pmol/(min \cdot mM)]$, is the rate of increase of the granular insulin available for secretion with increasing glycaemia.

Ghrelin, denoted as H (pg/ml) in the model, is secreted in the stomach but the signals that inhibit its production arise in response to food in the portion of the small

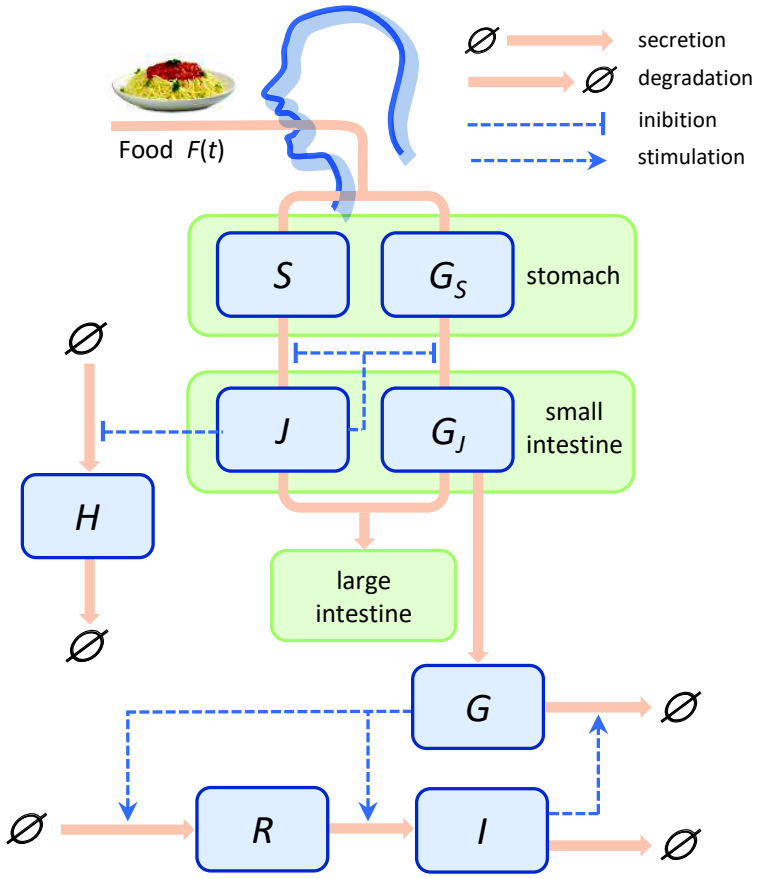

FIGURE 1. Graphical scheme of the model. Continuous lines represent transfer of mass, dashed lines represent signals.

intestine between the duodenum and the jejunum [31, 19]. This negative feedback is modelled by a decreasing exponential function depending on the content of the second gastrointestinal compartment, $J(t)$. Furthermore, a first order elimination rate of the hormone is also taken into account:

$$\dot{H}(t) = -k_{XH}H(t) + k_H(t)\frac{\mathrm{e}^{-\lambda_{HJ}J(t)}}{V_H} \tag{10}$$

where $k_H(t)$, $[pg/min]$, is the maximum rate of ghrelin secretion achieved when the jejunum is empty ($J(t) = 0$), λ_{HJ}, $[ml^{-1}]$, is the rate of decay of ghrelin secretion with jejunal filling, V_H, $[ml]$, is the ghrelin distribution volume, k_{XH}, $[min^{-1}]$, is the first order elimination rate for ghrelin. $k_H(t)$ is supposed to be vary with a 24h period, thus accounting for circadian variability. This fact is suggested by experimental evidence according to which ghrelin unexpectedly decreases in the hours before dawn without any meal assumption [3]. In the following we adopt a simple switching model for $k_H(t)$, from a maximum value k_H^{max} to a minimum value k_H^{min}, with the switch occurring at time t_H. Fig. 1 reports a block-diagram of the complete model.

3. **Qualitative analysis of the model.** In order to show the mathematical coherence of the model, main features of the qualitative analysis of the solutions are reported.

3.1. **Positivity of solutions.** In order to have physiological relevant results it is important that the model ensures non-negative solutions for the ODEs system, since the state variables describe the evolution of masses and concentrations. To prove it, we assume that the initial conditions are non-negative and that $F(t) \geq 0$, both physiologically meaningful assumptions.

Lemma 3.1. *The ODEs system (1)-(10) has non-negative solutions for any non-negative initial conditions and input.*

Proof. Consider the S dynamics and assume that $\exists\ \bar{t}$ such that $S(\bar{t}) = 0$ and $\dot{S}(\bar{t}) < 0$. This is a contradiction, since

$$\dot{S}(\bar{t}) = -\eta K_{JS}(\bar{t})S(\bar{t}) + k_S + F(\bar{t}) = k_S + F(\bar{t}) > 0$$

therefore $S(t) \geq 0\ \forall\ t \geq 0$. Analogously, it can be proven that also $G_S(t), H(t) \geq 0$.

Then consider the J dynamics and assume that $\exists\ \bar{t}$ such that $J(\bar{t}) = 0$ and $\dot{J}(\bar{t}) < 0$. This is a contradiction, since

$$\dot{J}(\bar{t}) = \eta(K_{JS}(\bar{t})S(\bar{t}) - k_{XJ}J(\bar{t})) + k_J = \eta K_{JS}(\bar{t})S(\bar{t}) + k_J$$

with $K_{JS}(\bar{t}) > 0$ because of its exponential fashion and $S(\bar{t}) \geq 0$ as previously proven. Then, also $J(t) \geq 0$. Analogously, it can be proven that also $G_J(t) \geq 0$. The positivity of J and G_J straightforwardly proves that $G(t) \geq 0$; this last finding proves that $R(t) \geq 0$ and, finally, that $I(t) \geq 0$. □

3.2. **Equilibrium point and stability analysis.** To discuss existence and stability of the equilibrium points, a constant input $F(t) \equiv \bar{F}$ is considered. It is possible to choice either $\bar{F} = 0$ (fasting situation) or a constant positive input, which could be the case of an experiment with gastric constant infusion of nutrients. Analogously, in this analysis, we consider a constant value for the switching parameter k_H (namely $\bar{k}_H$), which may be thought of as the maximum/minimum value.

Lemma 3.2. *The ODEs system (1)-(10) has a unique equilibrium point for $F(t) \equiv \bar{F}$.*

Proof. Denote with the suffix e all stationary variables, as well as $K_{JSe} = k_{JS}^{max} e^{-\lambda J_e}$. Then, the steady state equations are:

$$-\eta K_{JSe} S_e + k_S + \bar{F} = 0 \tag{11}$$

$$\eta(K_{JSe} S_e - k_{XJ} J_e) + k_J = 0 \tag{12}$$

$$-\eta K_{JSe} G_{Se} + \rho_{GM} \bar{F} = 0 \tag{13}$$

$$\eta(K_{JSe} G_{Se} - k_{XJ} G_{Je}) - k_{GJ} \frac{G_{Je}}{J_e} = 0 \tag{14}$$

$$\frac{k_G}{V_G} - k_{XGI} I_e G_e + k_{GJ} \frac{G_{Je}}{J_e V_G} = 0 \tag{15}$$

$$-k_{XI} I_e + k_{IRG} \left(\frac{G_e}{G_b}\right)^{\gamma_{IRG}} \frac{R_e}{V_I} = 0 \tag{16}$$

$$k_{RG} G_e - k_{IRG} \left(\frac{G_e}{G_b}\right)^{\gamma_{IRG}} R_e = 0 \tag{17}$$

$$-k_{XH}H_e + \bar{k}_H \frac{\mathrm{e}^{-\lambda_{HJ}J_e}}{V_H} = 0 \tag{18}$$

From these equations the following unique positive solution is achieved:

$$J_e = \frac{k_S + k_J + \bar{F}}{\eta k_{XJ}} \quad \Rightarrow \quad K_{JSe} \tag{19}$$

$$S_e = \frac{\bar{F} + k_S}{\eta K_{JSe}} \qquad G_{Se} = \frac{\rho_{GM}\bar{F}}{\eta K_{JSe}} \tag{20}$$

$$G_{Je} = \frac{\rho_{GM}\bar{F}}{k_{XJ} + \frac{k_{GJ}}{J_e}} \qquad G_e = \frac{k_{XI}V_I I_e}{k_{RG}} \tag{21}$$

$$I_e = \sqrt{\left(\frac{K_G}{V_G} + \frac{k_{GJ}G_{Je}}{J_e V_G}\right)\frac{k_{RG}}{k_{XGI}k_{XI}V_I}} \tag{22}$$

$$R_e = \frac{k_{XI}V_I I_e}{k_{IRG}}\left(\frac{G_b}{G_e}\right)^{\gamma_{IRG}} \qquad H_e = \frac{\bar{k}_H}{k_{XH}}\frac{\mathrm{e}^{-\lambda_{HJ}J_e}}{V_H} \tag{23}$$

□

In the case $F(t) \equiv 0$, i.e. fasting condition, the equilibrium values for the variables are their basal values in fasting conditions (with the trivial values $G_{Se} = 0$, $G_{Je} = 0$). In the following we analyze the stability of the equilibrium point: computations are carried out for the fasting condition, but results can be readily generalized for any value of $\bar{F}$. Dealing with basal conditions, the equilibrium suffix is changed from e into b. Looking for stability conditions, we study the eigenvalues of the Jacobian matrix, associated with the ODEs system (1)–(10), evaluated at the basal equilibrium point. From computations, non trivial entries of Jacobian matrix J are the following:

$$\begin{array}{lll}
J_{11} = -\eta K_{JSb} & J_{12} = \eta\lambda_{JS}K_{JSb}S_b & J_{21} = -J_{11} \\
J_{22} = -J_{12} - k_{XJ} & J_{33} = J_{11} & J_{43} = -J_{11} \\
J_{44} = -\eta k_{XJ} - \frac{k_{GJ}}{J_b} & J_{54} = \frac{k_{GJ}}{J_b V_G} & J_{55} = -k_{XGI}I_b \\
J_{56} = -k_{XGI}G_b & J_{65} = \frac{k_{IRG}\gamma_{IRG}R_b}{G_b V_I} & J_{66} = -k_{XI} \\
J_{67} = \frac{k_{IRG}}{V_I} & J_{75} = k_{RG} - J_{65}V_I & J_{77} = -k_{IRG} \\
J_{82} = -\frac{\bar{k}_H\lambda_{HJ}\mathrm{e}^{-\lambda_{HJ}J_b}}{V_H} & J_{88} = -k_{XH} &
\end{array}$$

Three of the eight eigenvalues can be easily deduced from the block-structure of the Jacobian matrix:

$$\lambda_3 = J_{33} < 0 \qquad \lambda_4 = J_{44} < 0 \qquad \lambda_8 = J_{88} < 0 \tag{24}$$

λ_1 and λ_2 are the eigenvalues of the following matrix:

$$A = \begin{bmatrix} -\eta K_{JSb} & \eta\lambda_{JS}K_{JSb}S_b \\ \eta K_{JSb} & -\eta\lambda_{JS}K_{JSb}S_b - k_{XJ} \end{bmatrix} \tag{25}$$

so that

$$\det(A) = \lambda_1\lambda_2 = \eta K_{JSb}k_{XJ} > 0 \tag{26}$$

whilst

$$\mathrm{tr}(A) = \lambda_1 + \lambda_2 = -\eta K_{JSb} - \eta\lambda_{JS}K_{JSb}S_b - k_{XJ} < 0 \tag{27}$$

That means: $\lambda_1, \lambda_2 < 0$.

λ_5, λ_6 and λ_7 are the eigenvalues of the following matrix:

$$B = \begin{bmatrix} -k_{XGI} I_b & -k_{XGI} G_b & 0 \\ \frac{k_{IRG}\gamma_{IRG} R_b}{G_b V_I} & -k_{XI} & \frac{k_{IRG}}{V_I} \\ k_{RG} - \frac{k_{IRG}\gamma_{IRG} R_b}{G_b} & 0 & -k_{IRG} \end{bmatrix} \tag{28}$$

We rewrite it as:

$$B = \begin{bmatrix} -a & -b & 0 \\ \frac{c}{V_I} & -d & \frac{e}{V_I} \\ k_{RG} - c & 0 & -e \end{bmatrix} \tag{29}$$

for appropriate choices of $a, b, c, d, e > 0$. Then, the characteristic polynomial of matrix (29) is:

$$\lambda^3 + (a + d + e)\lambda^2 + \left(\frac{bc}{V_I} + ad + ae + de\right)\lambda + \frac{bek_{RG}}{V_I} + ade \tag{30}$$

For the sake of simplicity, we rewrite (30) as:

$$\lambda^3 + h_1\lambda^2 + h_2\lambda + h_3, \qquad h_1, h_2, h_3 > 0 \tag{31}$$

It is possible to study the sign of the real part of the roots of the characteristic polynomial by means of the Routh-Hurwitz criterion. We use it in Lemma 3.3 in order to find a sufficient condition for the eigenvalues of matrix (29) to have negative real part.

Lemma 3.3. *The eigenvalues of matrix* (29) *have negative real part.*

Proof. Consider the Routh-Hurwitz table for the characteristic polynomial in (31):

$$\begin{array}{c|cc} 3 & 1 & h_2 \\ 2 & h_1 & h_3 \\ 1 & \frac{h_1 h_2 - h_3}{h_1} & 0 \\ 0 & h_3 & 0 \end{array} \tag{32}$$

The characteristic polynomial has all the roots with negative real part if and only if there are no sign variations in the first line of the table. Since $h_1, h_2 > 0$, to have no sign variations $h_1 h_2 > h_3$ must hold; thus:

$$\begin{aligned} &abc + bcd + bce + V_I ad^2 + V_I a^2 d + V_I ae^2 + V_I a^2 e + \\ &+ V_I de^2 + V_I d^2 e + 2V_I ade > bek_{RG} \end{aligned} \tag{33}$$

It is worth to notice that

$$V_I ade = bek_{RG} = k_{XGI} k_{XI} k_{IRG} I_b V_I, \tag{34}$$

so that (33) is always verified.

Since all the eigenvalues of the Jacobian matrix have negative real part, we can conclude that the fasting equilibrium point is asymptotically stable. □

4. **Model identification and numerical simulations.** The identification task has been carried out according to a set of experimental data coming from [3], referring to a 23-hour (6am-5am) experiment in which 10 healthy subjects were administered 3 meals approximating the average American diet. Ghrelin and insulin measurements were acquired at a sampling rate of 30min during daytime and 60min during nighttime. At each sampling instant the measurements taken on the 10 subjects are averaged. Thus, the only available data from [3] that can be used for model identification are average values and standard deviations. As a consequence,

the identified model is a sort of an average model of the system under investigation, not calibrated on a single subject. Unfortunately, no further experimental data are available for model validation.

Before to get into the details of the identification procedure, we briefly discuss the constraints on the values of some parameters that can be gathered from the available literature. Parameter ρ_{GM} in (5) is assumed to vary for the three kinds of meals according to the following expression

$$\rho_{GMi} = \frac{\alpha \cdot Ca \cdot M}{0.18} \cdot \frac{1}{V_{Mi}}, \qquad i = b, l, d, \tag{35}$$

where $V_{Mi} = r \cdot \tau_i$ is the meal volume (τ_i is the meal duration), different for the three meals (see (4)), $\alpha = 0.9$ is the glucose percentage in carbohydrates, Ca is the percentage of carbohydrates in the meal mass $M = 241.18g$ (each meal shares the same mass but different volumes) and 0.18 is a conversion factor providing *mmol* of glucose from g. Volumes V_G and V_I are expressed in liters. In order to exploit data from [22] where $[l/kgBW]$ had been adopted, we exploited the mean body weight BW, obtained from the BMI of the subjects in [3] and the average height of an American person [7]. With respect to the food intake, according to the experimental setting [3] (see also [23]) we set $\tau_b = 39min$, $\tau_l = 24min$, $\tau_d = 24.6min$, with $t_b = 8\text{am}$, $t_l = 12\text{am}$, $t_d = 17:30\text{pm}$.

Other parameters/initial conditions derived from the literature or constrained by the steady state conditions (hence not straightforwardly involved in the identification procedure) are reported in Table 1.

The identification procedure, exploiting the experimental data reported in [3], has been divided into three steps.

In the first step the parameters k_{JS}^{max}, k_S, k_J, λ_{JS}, k_{XJ}, k_H^{min}, k_H^{max}, t_H, λ_{HJ}, H_0 in Eqs. (1), (2), (10) have been estimated by minimizing the weighted mean squared error (MSE) between simulated and experimental ghrelin data:

$$M_H = \sum_{t_k \in \mathcal{S}_H} \frac{(H_m(t_k) - H(t_k))^2}{H_m(t_k)^2} \tag{36}$$

where $\mathcal{S}_H$ is the set of sampling-times for ghrelin measurements $H_m(t_k)$. The solution is achieved using the *ga* (genetic algorithm) and *fmincon* (constrained minimization) Matlab functions.

In the second step the procedure is repeated to estimate the parameters of the glucose-insulin subsystem (k_{GJ}, γ_{IRG}, G_0, R_0) by minimizing the weighted MSE

$$M_I = \sum_{t_j \in \mathcal{S}_I} \frac{(I_m(t_j) - I(t_j))^2}{I_m(t_j)^2}, \tag{37}$$

where $\mathcal{S}_I$ is the set of sampling-times for insulin measurements $I_m(t_j)$. In this phase the parameters computed in step 1 are kept constant. Again, the *ga* and *fmincon* Matlab functions have been used.

In the final step, the parameters estimated in steps 1-2 are used as a starting point for the Matlab *fmincon* function minimizing the overall MSE cost $M_H + M_I$, thus considering the whole system and all the available measurements (ghrelin and insulin) simultaneously.

The trick of resorting to steps 1 and 2 for finding a convenient initial guess to initialize the algorithm that finds the minimum of the MSE $M_H + M_I$ has avoided

TABLE 1. Model parameters and initial conditions.

Parameter	Units	Value	Reference
r	ml/min	35	[23]
k_{JS}^{max}	min^{-1}	0.0201	Identification
λ_{JS}	min^{-1}	$9.1871 \cdot 10^{-4}$	Identification
k_S, k_J	mml/min	6.2568	Identification
k_{XJ}	min^{-1}	0.0737	Identification
Ca	$-$	0.5558	[3]
k_{GJ}	ml/min	50.1503	Identification
k_G	$mmol/min$	0.2066	Steady State
V_G	l	10.483	[22]
BW	kg	68.97	[3, 7]
k_{xGI}	min^{-1}	$5.3 \cdot 10^{-5}$	[22]
k_{IRG}	min^{-1}	0.0049	Steady state
γ_{IRG}	$-$	3.0763	Identification
$V_I = V_H$	l	17.2425	[22]
k_{xI}	min^{-1}	0.059	[21]
k_{RG}	min^{-1}	17.6948	Steady state
k_H^{min}	$pmol/ml$	650407.4627	Identification
k_H^{max}	$pmol/ml$	899990.4238	Identification
t_H	$pmol/ml$	1195.2917	Identification
λ_{HJ}	min^{-1}	0.007	Identification
k_{XH}	l	0.239	[1]
S_0	ml	363.3046	Steady state
J_0	ml	169.8402	Steady state
G_{S0}	$mmol$	0	Steady state
G_{J0}	$mmol$	0	Steady state
$G_0 = G_b$	mM	4.6239	Identification
I_0	pM	80.4264	[3]
R_0	$pmol$	16581.6656	Identification
H_0	pg/ml	524.5618	Identification

the convergence of the algorithm to local minima. Fig. 2 shows the quality of the fit: the simulated curves reproduce with good accuracy the experimental data.

Unfortunately, the set of experimental data coming from [3] does not include any further useful information (e.g. glucose behavior, or data from another independent experiment). For this reason, the model can be validated only from a qualitative behavior perspective, i.e. the ability to reproduce physiologically meaningful behaviors. To this end, we report the plots of the gastrointestinal emptying and the glucose dynamics in Figs. 3-4. It is worthwhile to notice that the first gastrointestinal compartment empties almost completely in 4 hours, in agreement with experimental evidence for stomach emptying [26] (less than 5% of total ingested food at breakfast is still in the stomach at noon). Furthermore, the glucose behavior is physiologically consistent, oscillating above its basal value during the day due to meal ingestions counteracted by fast insulin action.

In order to further underline the role of ghrelin in meal initiation, we simulated the ghrelin dynamics in a day during which breakfast and dinner are as in [3], but no lunch has been served. As shown in Fig. 5, ghrelin reaches a higher peak than in the previous case, which may explain the sense of hunger following a prolonged

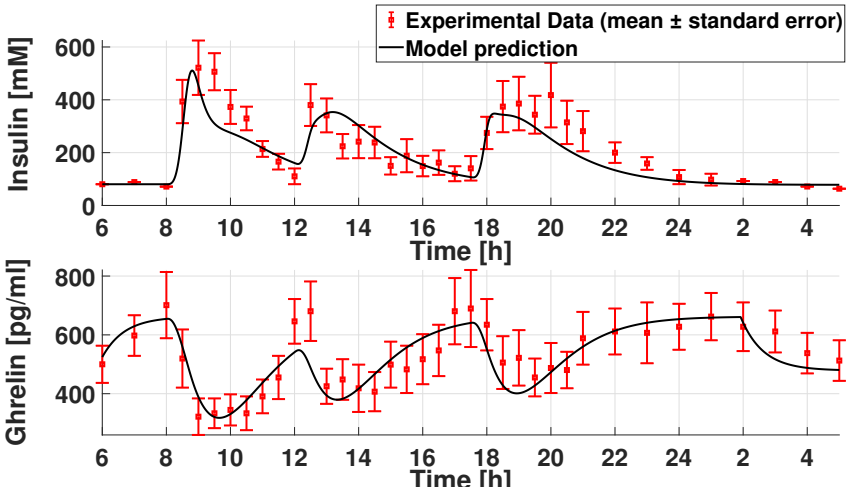

FIGURE 2. Plasma insulin and ghrelin evolutions

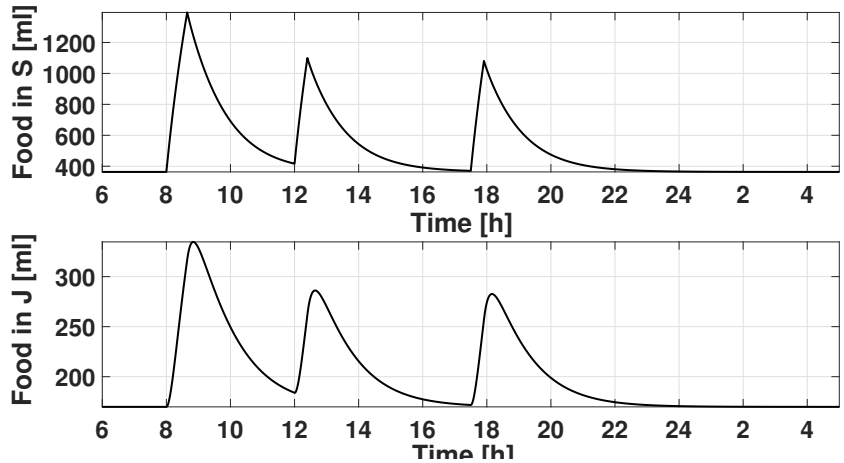

FIGURE 3. Food volume in the gastrointestinal tract dynamics

fasting. High ghrelin levels may activate processes that lead to meal initiation, and this explains the role of ghrelin as a survival hormone [3, 14].

5. **Conclusions.** This note presents a multi-compartment mathematical model of food intake that accounts for glucose-insulin homeostasis and ghrelin dynamics. The model is grounded in the established physiology and the qualitative behavior analysis shows that its solutions are mathematically consistent. The fitting to clinical experimental data is good and provide physiologically meaningful time evolutions for the all state variables.

The model paves the way to further long-term descriptions of metabolic regulation and body weight dynamics, extending to human models the work [10] focusing on rats.

A further improvement could be to consider the effect of insulin on ghrelin secretion. There are conflicting experimental results on this topic in the literature;

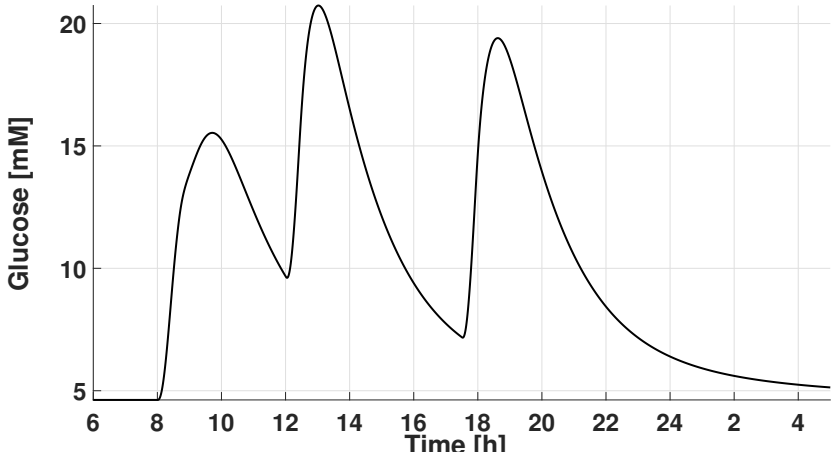

FIGURE 4. Plasma glucose dynamics

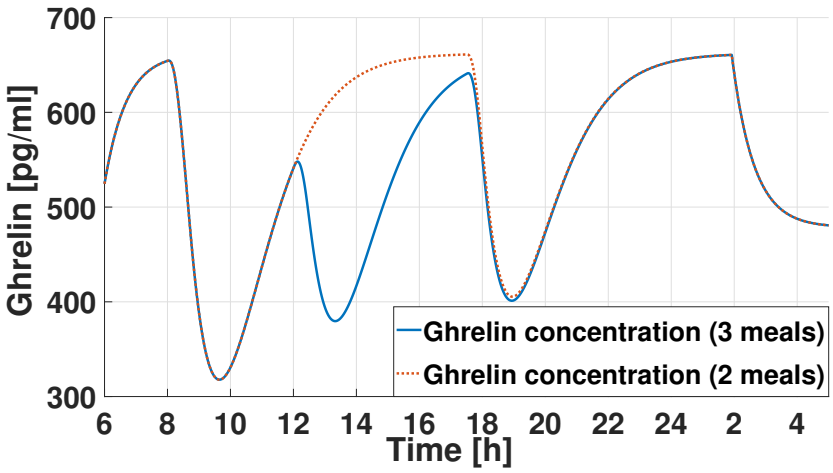

FIGURE 5. Ghrelin dynamics in a day with 3 and with 2 meals

some findings, indeed, suggest that insulin inhibits ghrelin production whilst others come to the opposite conclusion, conjecturing that ghrelin is stimulated by insulin [34]. By using mathematical modeling, both the hypotheses might be investigated, shedding light on the problem.

REFERENCES

[1] T. Akamizu, K. Takaya, T. Irako, H. Hosoda, S. Teramukai, A. Matsuyama, H. Tada, K. Miura, A. Shimizu, M. Fukushima, et al., Pharmacokinetics, safety, and endocrine and appetite effects of ghrelin administration in young healthy subjects, *European Journal of Endocrinology*, **150** (2004), 447–455.

[2] S. L. Aronoff, K. Berkowitz, B. Shreiner and L. Want, Glucose metabolism and regulation: Beyond insulin and glucagon, *Diabetes Spectrum*, **17** (2004), 183–190.

[3] D. E. Cummings, J. Q. Purnell, R. S. Frayo, K. Schmidova, B. E. Wisse and D. S. Weigle, A preprandial rise in plasma ghrelin levels suggests a role in meal initiation in humans, *Diabetes*, **50** (2001), 1714–1719.
[4] D. E. Cummings, Ghrelin and the short-and long-term regulation of appetite and body weight, *Physiology & Behavior*, **89** (2006), 71–84.
[5] D. E. Cummings, D. S. Weigle, R. S. Frayo, P. A. Breen, M. K. Ma, E. P. Dellinger and J. Q. Purnell, Plasma ghrelin levels after diet-induced weight loss or gastric bypass surgery, *New England Journal of Medicine*, **346** (2002), 1623–1630.
[6] D. E. Cummings and M. H. Shannon, Roles for ghrelin in the regulation of appetite and body weight, *Archives of Surgery*, **138** (2003), 389–396.
[7] C. D. Fryar, Q. Gu, C. L. Ogden and K. M. Flegal, Anthropometric reference data for children and adults; united states, 2011-2014, *Vital Health Stat*, **3** (2016), 1–46.
[8] J. C. Hou, L. Min, J. E. Pessin and Insulin granule biogenesis, trafficking and exocytosis, *Vitamins & Hormones*, **80** (2009), 473–506.
[9] J. Hunt, J. Smith and C. Jiang, Effect of meal volume and energy density on the gastric emptying of carbohydrates, *Gastroenterology*, **89** (1985), 1326–1330.
[10] M. Jacquier, F. Crauste, C. O. Soulage and H. A. Soula, A predictive model of the dynamics of body weight and food intake in rats submitted to caloric restrictions, *PLoS One*, **9** (2014).
[11] G. L. Kellett and P. A. Helliwell, The diffusive component of intestinal glucose absorption is mediated by the glucose-induced recruitment of glut2 to the brush-border membrane, *Biochemical Journal*, **350** (2000), 155–162.
[12] G. L. Kellett, The facilitated component of intestinal glucose absorption, *The Journal of Physiology*, **531** (2001), 585–595.
[13] P. Maljaars, H. Peters, D. Mela and A. Masclee, Ileal brake: A sensible food target for appetite control. a review, *Physiology & Behavior*, **95** (2008), 271–281.
[14] B. K. Mani and J. M. Zigman, Ghrelin as a survival hormone, *Trends in Endocrinology & Metabolism*, **28** (2017), 843–854.
[15] T. H. Moran and K. P. Kinzig, Gastrointestinal satiety signals ii. cholecystokinin, *American Journal of Physiology-Gastrointestinal and Liver Physiology*, **286** (2004), G183–G188.
[16] J. Moore, P. Christian and R. Coleman, Gastric emptying of varying meal weight and composition in man, *Digestive Diseases and Sciences*, **26** (1981), 16–22.
[17] M. Nakazato, N. Murakami, Y. Date, M. Kojima, H. Matsuo, K. Kangawa and S. Matsukura, A role for ghrelin in the central regulation of feeding, *Nature*, **409** (2001), 194–198.
[18] D. L. Nelson, M. M. Cox and A. L. Lehninger, *Principles of Biochemistry*, Freeman New York, 2008.
[19] J. Overduin, R. S. Frayo, H. J. Grill, J. M. Kaplan and D. E. Cummings, Role of the duodenum and macronutrient type in ghrelin regulation, *Endocrinology*, **146** (2005), 845–850.
[20] P. Palumbo, S. Ditlevsen, A. Bertuzzi and A. De Gaetano, Mathematical modeling of the glucose–insulin system: A review, *Mathematical Biosciences*, **244** (2013), 69–81.
[21] P. Palumbo, S. Panunzi and A. De Gaetano, Qualitative behavior of a family of delay-differential models of the glucose-insulin system, *Discrete Contin. Dyn. Syst. Ser. B*, **7** (2007), 399–424.
[22] S. Panunzi, P. Palumbo and A. De Gaetano, A discrete single delay model for the intra-venous glucose tolerance test, *Theoretical Biology and Medical Modelling*, **4** (2007), 35.
[23] J. Pires, A. Borri, A. De Gaetano, C. Manes and P. Palumbo, A short-term dynamical model for ghrelin, *IFAC-PapersOnLine*, **50** (2017), 11011–11016.
[24] J. G. Pires, Some insights into an integrative mathematical model: A prototype-model for bodyweight and energy homeostasis, *Revista Eletrônica Gestão e Saúde*, **3** (2016), 1271–1288.
[25] P. V. Röder, K. E. Geillinger, T. S. Zietek, B. Thorens, H. Koepsell and H. Daniel, The role of SGLT1 and GLUT2 in intestinal glucose transport and sensing, *PloS One*, **9** (2014).
[26] D. E. Sadava, D. M. Hillis, H. C. Heller and M. Berenbaum, *Life: The Science of Biology*, Vol. **2**, Macmillan, 2009.
[27] S. Stanley, K. Wynne and S. Bloom, Gastrointestinal satiety signals iii. glucagon-like peptide 1, oxyntomodulin, peptide yy, and pancreatic polypeptide, *American Journal of Physiology-Gastrointestinal and Liver Physiology*, **286** (2004), G693–G697.
[28] R. E. Steinert, C. Feinle-Bisset, L. Asarian, M. Horowitz, C. Beglinger and N. Geary, Ghrelin, cck, glp-1, and pyy(3–36): Secretory controls and physiological roles in eating and glycemia in health, obesity and after rygb, *Physiol Rev*, **97** (2017), 411–463.

[29] P. Toghaw, A. Matone, Y. Lenbury and A. De Gaetano, Bariatric surgery and t2dm improvement mechanisms: A mathematical model, *Theoretical Biology and Medical Modelling*, **9** (2012), 16.
[30] C. Uluseker, G. Simoni, L. Marchetti, M. Dauriz, A. Matone and C. Priami, A closed-loop multi-level model of glucose homeostasis, *PloS one*, **13** (2018), e0190627.
[31] D. L. Williams, D. E. Cummings, H. J. Grill and J. M. Kaplan, Meal-related ghrelin suppression requires postgastric feedback, *Endocrinology*, **144** (2003), 2765–2767.
[32] E. M. Wright, M. G. Martìn and E. Turk, Intestinal absorption in health and disease-sugars, *Best Practice & research Clinical Gastroenterology*, **17** (2003), 943–956.
[33] E. M. Wright, M. Sala-Rabanal, C. Ghezzi and D. D. Loo, Sugar absorption, in: *Physiology of the Gastrointestinal Tract*, Elsevier, 2018, 1051–1062.
[34] X. Yin, Y. Li, G. Xu, W. An and W. Zhang, Ghrelin fluctuation, what determines its production?, *Acta Biochimica et Biophysica Sinica*, **41** (2009), 188–197.

Received for publication December 2020.

E-mail address: mas.barnabei@gmail.com
E-mail address: alessandro.borri@biomatematica.it
E-mail address: andrea.degaetano@biomatematica.it
E-mail address: costanzo.manes@univaq.it
E-mail address: pasquale.palumbo@unimib.it
E-mail address: jorgeguerrabrazil@gmail.com